NUMERICAL STUDY ON ONE-DIMENSIONAL INCOMMENSURATE CHAGE-DENSITY-WAVES IN THE WEAK PINNING REGIME(THEORIES ON CDW NONLINEAR DYNAMICS, International Symposium on NONLINEAR TRANSPORT AND RELATED PHENOMENA IN INORGANIC QUASI ONE DIMENSIONAL CONDUCTORS)

AUTHOR(S):

TAKAYAMA, Hajime; MATSUKAWA, Hiroshi

NUMERICAL STUDY ON ONE-DIMENSIONAL INCOMMENSURATE CHAGE-DENSITY-WAVES IN THE WEAK PINNING REGIME

Hajime TAKAYAMA and Hiroshi MATSUKAWA
Department of physics, Hokkaido University,
Sapporo 060, Japan

We show in this work by the joint use of the Monte Carlo and molecular dynamics techniques that a classical treatment of the Fukuyama-Lee model on 1D incommensurate CDW in the weak pinning regime can well reproduce the peculiar transport properties attributed to a motion of CDW, such as the nonlinear electric conduction associated with narrow band noises. The results of the inspection of phase profiles in motion are also discussed.

The Fukuyama-Lee theory[1,2] on 1D incommensurate CDW condensate describes behavior of CDW in terms of its phase variable $\phi(x,t)$, while its amplitude is held constant. The FL energy for $\phi(x)\to\phi_\ell$ on a discretized (d-) lattice introduced for numerical simulation is written as

$$\frac{E^{FL}}{E_e} = \frac{1}{2c}\sum_{\ell=1}^{M}(\phi_\ell-\phi_{\ell-1})^2 + \varepsilon_i\sum_{\ell_j=1}^{N_i}\cos(Qd\ell_j+\phi_{\ell_j}) - \varepsilon_f\sum_{\ell=1}^{M}\phi_\ell \qquad (1)$$

where $E_e=v_F n_i/2\pi$, $c=N_i/M=n_i d$, $\varepsilon_i=V_0\rho_0/E_e$ and $\varepsilon_f=eE/\pi n_i E_e$. Here $n_i=N_i/L$ is the impurity density, N_i being the number of impurities and L the system size. M, d, c and ℓ_j are the quantities related to the d-lattice; M being the number of its sites, d its lattice distance, c the impurity concentration on this lattice, and ℓ_j the impurity sites. The other notations are the same as in the FL paper[2] (see also Teranishi and Kubo[3]). The first two

terms in r.h.s. of Eq.(1) are the elastic and impurity potential energies, E_{ela} and E_{pot}, respectively, and the last term is the electric field energy with ε_f being the reduced field strength. The parameter $\varepsilon_i (\equiv 2\pi\varepsilon)$, where ε is the corresponding parameter in the FL theory, specifies whether CDW is in the weak ($\varepsilon<1$) or strong ($\varepsilon>>1$) pinning regime. In the present work we exclusively study systems with $\varepsilon_i=1$. Also we examine only systems with $c=1/4$. This value is chosen because, on the one hand, d has to be much smaller than ξ^{FL}, the coherence length in the $\phi(x)$ variation given by[2)]

$$\xi^{FL} = \left(\frac{2}{\alpha\varepsilon_i}\right)^{2/3} n_i^{-1} \qquad (2)$$

with $\alpha=3/\pi^2$ ($\xi^{FL}\simeq 14d$ with $\varepsilon_i=1$ and $c=1/4$), but on the other hand, accurate numerical simulation is the harder for systems with the smaller c.

We have carried out the MC simulation[4)] on 2(5) samples with $N_i=250(50)$ to look for their equilibrium configurations of E^{FL}. The samples have the same parameters specified above, but have different sets of ℓ_j. The periodic boundary condition $\phi_M=\phi_0$ is imposed on them. For each system many equilibrium configurations

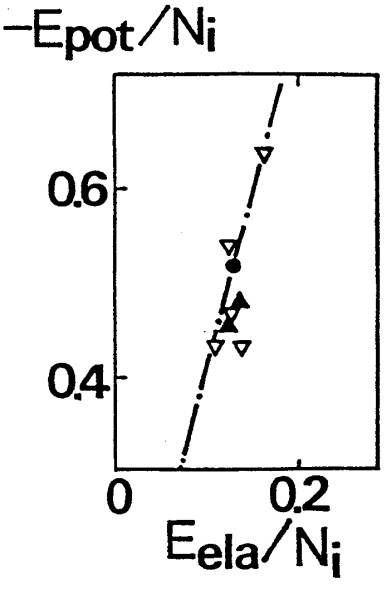

Fig. 1. $-E_{pot}$ vs E_{ela} of the lowest energy configurations of our seven samples. The chain line represents $E_{pot}=-4E_{ela}$, and the solid circle is the FL value with $\alpha=3/\pi^2$.

are found. Plotted in Fig. 1 are $-E_{pot}$ vs. E_{ela} of the lowest energy state found within our simulation for each sample with $\varepsilon_f=0$. The results confirm the FL theory on the weakly pinned CDW, according to which the energies are given by $-E_{pot}=4E_{ela}=(\alpha/2)^{1/3}N_i$, where $E_e=1$ and $\varepsilon_i=1$ are used to derive the last equality. By the inspection of phase profiles the existence of ξ^{FL}, whose magnitude agrees with Eq. (2) within a few factor, is also ascertained. For an example we show in Fig. 2 the relative phase shift from one of the equiliblium configurations with $\varepsilon_f=0$ observed when the field less than ε_f^T, the threshold field, is applied and then switched off. The value ε_f^T of each sample can be determined by the MC method within an accuracy of ± 0.025 from the criterion whether stable solutions exist or the phases are

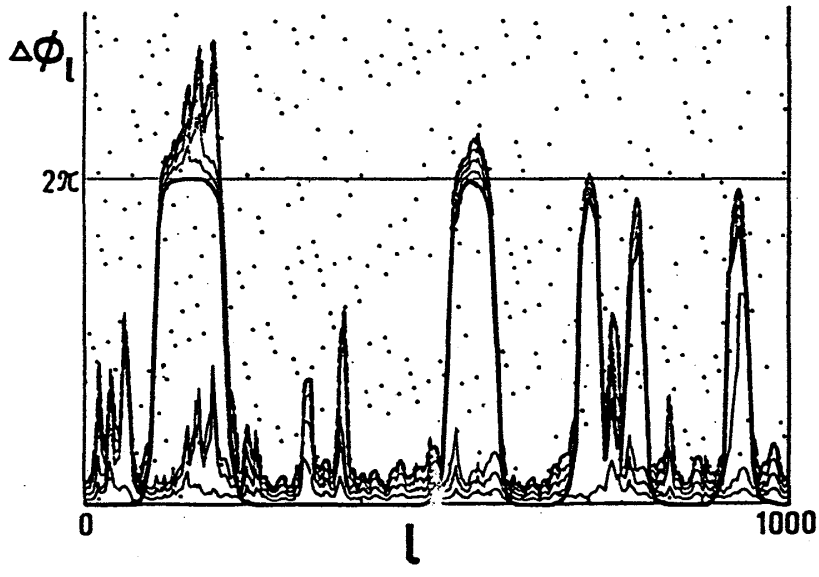

Fig. 2. An example of the relative phase shifts from one of the equilibrium configurations with $\varepsilon_f=0$ when the field $\varepsilon_f=0.2$ ($<\varepsilon_f^T$) is applied and then switched off. The dotts represent ϕ_{lj} at which the impurity potential is maximum. The configurations at $\varepsilon_f=0.2$ (broken curve) and at $\varepsilon_f=0$ after the switching off (solid curve) are stable our MC observation at T=0.

ever increasing (i.e., the CDW is sliding).

Switching on the field larger than ε_f^T upon the equilibrium configuration thus obtained, we examine dynamics of the sliding CDW by the MD technique based on the following equation of motion for ϕ_ℓ[3)]

$$\Gamma^2(\ddot{\phi}_\ell+\dot{\phi}_\ell) = \phi_{\ell-1}-2\phi_\ell+\phi_{\ell+1} + c\varepsilon_i \sum_{\ell_j} \sin(Qd\ell_j+\phi_{\ell_j})\delta_{\ell,\ell_j} - c^2\varepsilon_f \qquad (3)$$

where $\Gamma=d\gamma/v$, v being the phason velocity.[2)] To derive Eq. (3) we have introduced a phenomenological frictional force proportional to $-\gamma\dot{\phi}_\ell$, and normalized the time by γ^{-1}, or $\gamma t\to t$. In the present work we put $\Gamma^2=10$, which corresponds to the overdamped regime of the ϕ_ℓ-dynamics. Equation (3) is solved by means of the Runge-Kutta argebra with the (normalized) time step of $\Delta t=0.5$. The current associated with the sliding CDW is then evaluated by $J(t)=(e/\pi M)\Sigma\dot{\phi}_\ell$.

The clude value of ε_f^T of each sample is obtained by the MC method as mentioned above. We have then tried to adjust it

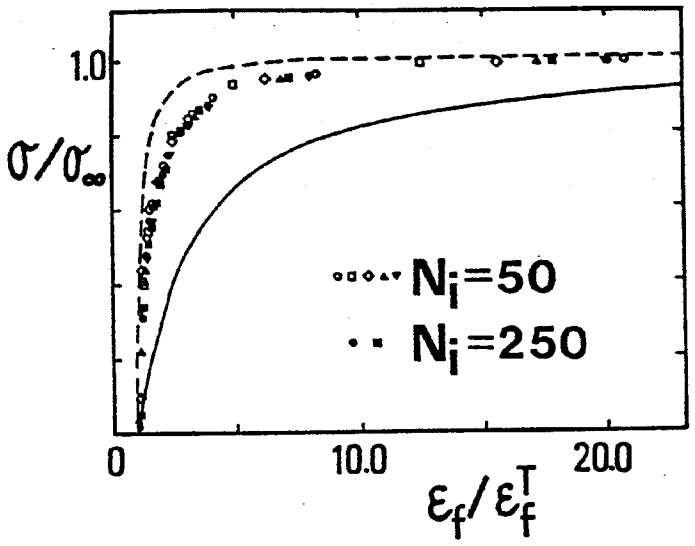

Fig. 3. The static nonlinear conductivities of our seven samples. The solid and broken curves indicate those obtained by Bardeen's tunneling theory[9)] and by the classical particle model with a sinusoidal potential,[10)] respectively.

slightly whether the normalized static conductivity $\sigma(\varepsilon_f)/\sigma(\infty)$ plotted against $\varepsilon_f/\varepsilon_f^T$ of the seven samples lie on a common curve. The results are shown in Fig. 3, with $\varepsilon_f^T \simeq 0.25 \sim 0.45$, which are somewhat larger than those obtained previously.[3,5] It is noted here that even with a relatively large $\varepsilon_f (\simeq 1)$ the prefactor of the last term in Eq.(1) or (3) is rather small compared with those of the rest. This means that appropriate equilibrium configurations determined through E_{ela} and E_{pot} are indispensable to examine subtle field effects. In this respect the present joint use of the MC and MD techniques is much advantageous than the previous work,[3,5,6] Unfortunately, however, it is still hard to simulate the fine details of $\sigma(\varepsilon_f)$ just above ε_f^T.

The current J(t) exhibits a certain periodic structure as shown in Fig. 4. Its period turns out the time for $\phi (\equiv M^{-1}\Sigma\phi_\ell)$ to increase by 2π. Therefore its inverse, i.e., the fundamental frequency Ω of the narrow band noise, is proportional to the static (averaged over t) current as found experimentally. This is confirmed by the direct inspection of J(t) when $\varepsilon_f > 2\varepsilon_f^T$. For ε_f near above ε_f^T, however, the structure of J(t) becomes complicated as seen in Fig. 4b. In this case an interesting result is found in the phase profiles in motion as shown in Fig. 5b: the overall phase increases inhomogeneously, i.e., by the local movement of solitons and antisolitons,[4] and by their pair creation or annihilation. These inhomogeneities are thought to yield a fine structure in J(t). When $\varepsilon_f >> \varepsilon_f^T$, on the contrary, the overall phase increases rather homogeneously as shown in Fig. 5a, resulting very sharp peaks at Ω and its higher harmonics in the noise spectrum. Further analysis on the spectra is now in progress.

Finally we note other interesting phenomena found in the present simulation. i) The amplitude of the current noise seems to decrease as the time proceeds. This has been clearly observed when $\varepsilon_f > 10\varepsilon_f^T$. ii) Responses of the current to pulsed fields are also examined. As expected from our choice of Γ no inductive (inertia) effect is observed just after the switching on or off of the field. iii) The phase profile after the switching off the

field is clearly different from that before applying the field. (By our simulation this is also the case even with ε_f less than ε_f^T as seen in Fig. 2.) This is certainly related to some hysteretic phenomena observed experimentally.[7] However no systematic "overshooting" phenomena have not yet been observed. iv) The total (impurity) force acting on the whole CDW, $c\varepsilon_i \Sigma_j \sin(Qd\ell_j + \phi_{\ell j})$, decreases as ε_f above ε_f^T increases. This indicates that when one tries to interpret the present results by means of the

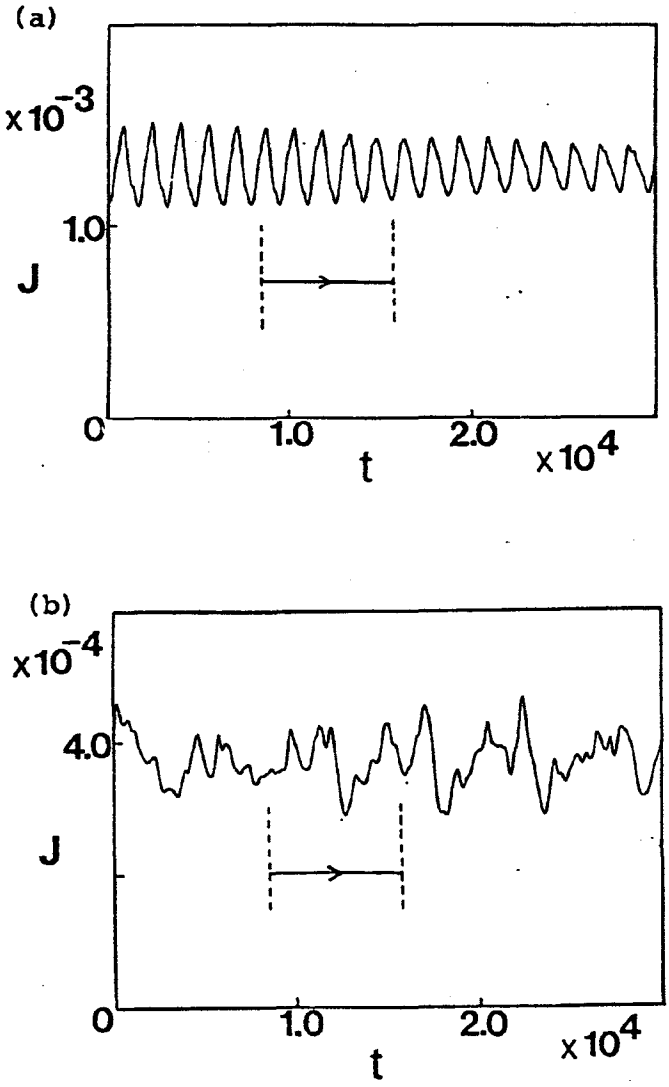

Fig. 4. Real-time current profiles of one sample with N_i= 250 under

a) ε_f=0.8=2.9ε_f^T

b) ε_f=0.4=1.4ε_f^T.

See Fig. 5 as for the meaning of the arrows.

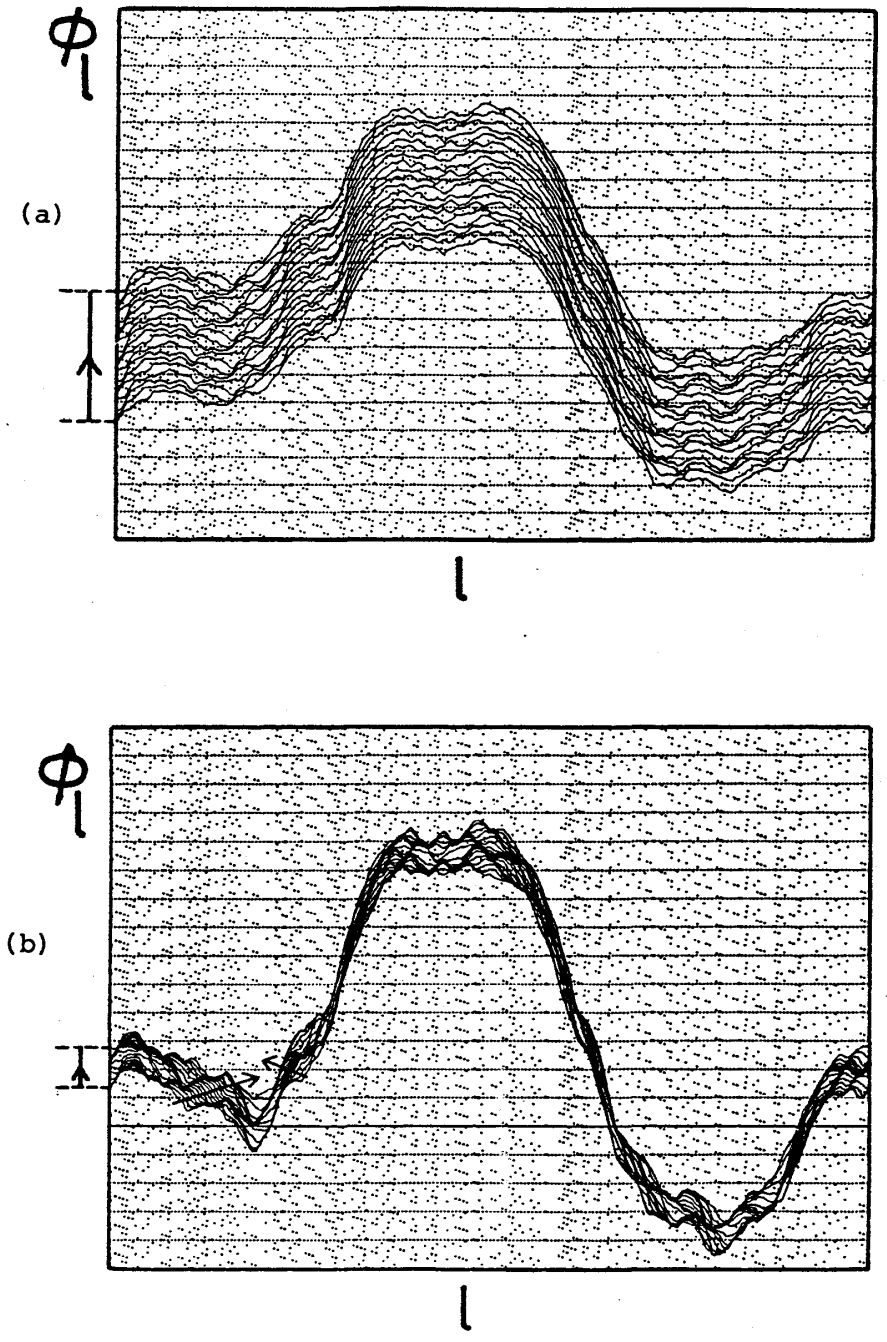

Fig. 5. The corresponding phase profiles in motion at the time intervals indicated by the arrows in Fig. 4 under ε_f=0.8 (a) and ε_f=0.4(b). Notice the local movement of solitons and antisolitons as indicated by the arrows in (b).

single particle model for a whole CDW, the force (and so potential) acting on the particle has to depend on the field.

In conclusion we have confirmed by numerical study that the literal FL model on 1D incommensurate CDW condensate in the weak pinning regime and with a large phenomenological frictional force does reproduce many interesting transport phenomena, which are observed experimentally in some quasi-1D conductors. They are attributed to the CDW sliding motion. Dynamics of the CDW phase profiles, i.e., that of the internal degrees of freedom of CDW, is shown to play an important role on these phenomena. To explain experimental results much closely, however, some refinements of the FL model are certainly required, such as to include the distribution of ε_i,[8] or the 2D or 3D character.

The authors would like to thank Profs. T. Sambongi and M. Ido, and Mr. M. Oda for informative discussions about experiments on the sliding CDW. Numerical calculation was made by Hitac M-280H at Hokkaido University Computing Center. This work was financially supported partially by Mitsubishi Science Foundation.

References

1) H. Fukuyama: J. Phys. Soc. Jpn. 41, 513 (1976).
2) H. Fukuyama and P. A. Lee: Phys. Rev. B17, 535 (1978).
3) N. Teranishi and R. Kubo: J. Phys. Soc. Jpn. 47, 720 (1979).
4) P. B. Littlewood and T. M. Rice: Phys. Rev. Lett. 48, 44 (1982).
5) L. Pietronero and S. Strässler: preprint.
6) J. B. Sokoloff: Phys. Rev. B23, 1992 (1981).
7) J. C. Gill: Solid State Commun. 39, 1203 (1981).
8) D. S. Fisher: Phys. Rev. Lett. 50, 1486 (1983).
9) J. Bardeen: Phys. Rev. Lett. 42, 1498 (1979), 45, 1978 (1980).
10) G. Grüner, A. Zawadowski and P. M. Chaikin: Phys. Rev. Lett. 46, 511 (1981).